Chapter - 3

Design of Test Rig for Macro Scaled Flagella

3.1 Introduction

In the previous chapter, comprehensive literature review including macro scale artificial nanoswimmer swimmer as well as different propulsion mechanism of micro/nano scale artificial swimmer is presented chronologically. Enhancement in propulsive force through various designs of macro scaled flagellated artificial swimmer is the main objective of the thesis. A literature survey on experimental investigation at scaled up level by utilizing planar and helical mode of propulsion are described in the earlier chapter. In the vast literature, researchers have worked on constant diameter flagellum, tapered flagellated nanoswimmer but effect of branches is not considered yet. *Ochrophyte* is a genus of algae whose flagellum is covered by hair like vertical appendages called as mastigonemes. In the present chapter, the branches (mastigonemes) on flagella are employed for designing of tail of an artificial swimmer and experiments are performed at macro-scale in silicon oil medium to maintain low Reynolds number to capture swimming environment around bacteria. The effects of branches on generation of thrust force is investigated by fabricating the branched flagella using flexible PDMS (polydimethylsiloxane) biocompatible material suitable for human body and biological applications, and resulting data are quantitatively compared through statistical analysis in the next chapter.

As a first problem at hand, in an attempt to propel artificial nanoswimmer, the design is scaled up using dimensionless theorem (Buckingham Pi theorem). Two modes of propulsion namely planar and helical mode of propulsion exhibit in nature by eukaryotic and prokaryotic bacteria. In the present study, the planar mode of propulsion of artificial nanoswimmer is investigated at scaled up level using scotch yoke mechanism. In the subsequent sections, we discuss the Buckingham Pi theorem, design of test rig at macro scale and fabrication process of different designs of scaled up artificial swimmer. The system parameters such as speed of motor, viscosity of fluid medium and different geometries of swimmer are explained with effect of branches.

3.2 Design of Test Bench Set-up

The following section includes the determination of scaling parameters, mould dimensions, tail fabrication and propulsive force measurement. The different designs of flagellated artificial swimmer are obtained by varying the number of branches (n), the orientation of branches (θ) with respect to flagella and the spacing between two consecutive branches (δ). The experimental investigations [1],[2] attempted, to establish a theory, are conducted with rigid flagella at scaled up dimensions. To develop suitable test bench system for propulsion of artificial swimmer at macro scale, kinematic and dynamic similarity has to be maintained in between scaled up model and actual nano size model.

To explore propulsive characteristics of artificial nanoswimmer at scaled up level, researchers have used planar and helical mode of propulsion. In 2006, Tony et al. [3] investigated first time planar mode of propulsion of macro swimmer using scotch yoke mechanism with rigid tail. A DC geared motor attached to cantilever beam has been used to oscillate stainless steel wire as flagella of length 18 to 30 cm. Experiments have been carried out in silicone oil medium to maintain Reynolds number in the range (10^{-2} to 10^{-4}). Strain gauges were used to measure deflection of cantilever beam generated due to oscillation of rigid tail as shown in Figure 3.1.

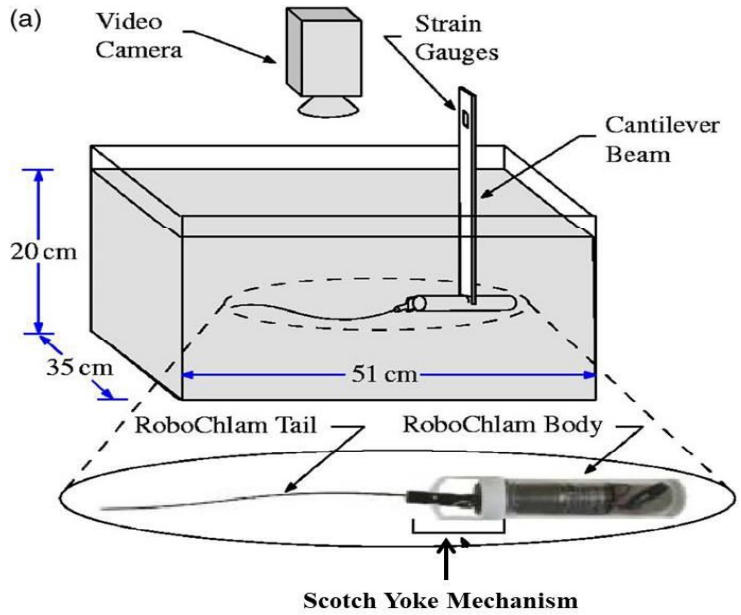

Figure 3.1: Planar oscillation of flagella through scotch yoke mechanism [3]

In 2006, Behkam and Sitti [4] proposed a scaled up model of swimming robot using Buckingham Pi theorem in silicon oil medium to maintain low Reynolds number condition. Stepper motor is used for rotating helical flagellum made up of steel wires of different size and wavelength as shown in Figure 3.2(a). In 2019, Danis et al. [5] studied the single as well as multi-helical flagellum to understand propulsive mechanics. Helical propulsion at scaled up level is also endeavored by Singleton et al. [6] in 2011. The thrust force was measured by monitoring deflection of cantilever beam due to rotating helical flagella through load cells. The experimental set up is shown in Figure 3.2(b). In both the experimental set ups, the rotating helical flagella was immersed in highly viscous silicon oil to maintain low Reynolds number flow condition at macro scale.

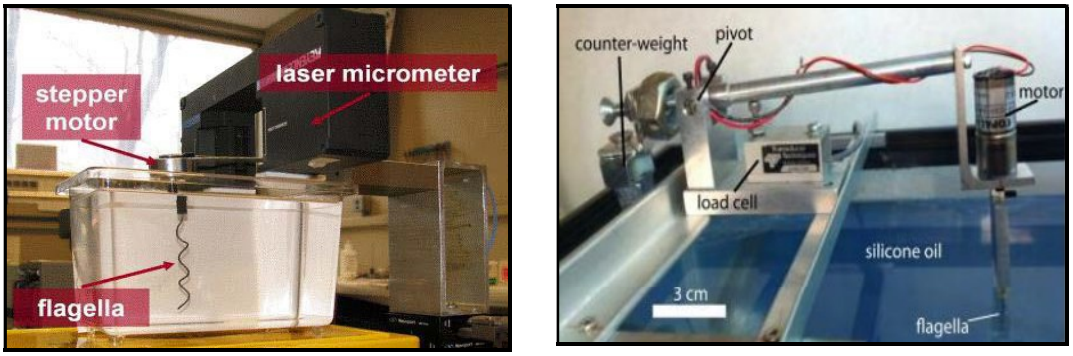

(a) (b)

Figure 3.2: (a) and (b) shows macro scaled experiments performed with helical propulsion mode [4], [6]

The thrust force is being measured for both planar and helical mode of propulsion through cantilever beam defection but all the attempts have been made at rigid flagella. The work presented, is the first attempt towards development of flexible flagella fabricated from biocompatible material. Thus test rig of macro flagellated swimmer is designed to reconnoiter the behavior of the system proposed here. Due to intricacy in exploiting absolute swimming nanorobots, it is determined that test bench will use a fixed body. Consequently, swimming velocity is zero and the propulsive force is measured. To design a test rig, system is scaled up using Buckingham Pi theorem as being discussed below along with scotch yoke mechanism to exhibit planar motion by fabricated branched flagellated nanoswimmer using PDMS biocompatible material.

3.2.1 System scale

A flexible filament at micron level is not possible to fabricate using common manufacturing technique. Also, absolute planar actuation system cannot be easily observed. The forces produced by micron level organism are small enough that would be challenging to measure. To eradicate these difficulties, the size of the system design is scaled up to manageable level.

However, scaling of the geometric parameters cannot be ensured without varying the other system parameters. However, the same scaling cannot be applied experimentally because of real world constraints. The dimensional analysis is a technique to predict physical parameters that influence the fluid flow around the swimmer elastic tail is used. The basic theorem of dimensional analysis is called as Buckingham Pi theorem. The dimensionless quantities are called the Pi (π) terms.

In terms of experimental corroboration, the useful characteristic of the Pi terms is their resemblance among system of different scales. Emergent of physical system at original scale is bit challenging. Though, it is postulated that the system can be developed, represented by the letter *X*, and illustrated by the following Pi terms:

$$\pi_{1X} = \phi(\pi_{2X}, \pi_{3X}, ...\pi_{nX}) \tag{3.1}$$

where, π_{1X} is a function (ϕ) of the other Pi terms. Now, consider the scaled up form of equivalent system, symbolized by the letter *Y*, and illustrated by the following term:

$$\pi_{1Y} = \phi(\pi_{2Y}, \pi_{3Y}, ...\pi_{nY}) \tag{3.2}$$

Under the subsequent conditions of dynamic similarity:

$$\pi_{2X} = \pi_{2Y},$$
$$\pi_{3X} = \pi_{3Y},$$

$$\pi_{nX} = \pi_{nY}.$$

and considering that the form of ϕ is similar for both the systems, it ensues that:

$$\pi_{1X} = \pi_{1Y} \tag{3.3}$$

Hence, denoting that the computed value of π_{1Y} acquired from system *Y* will be equal to the corresponding π_{1X} of system *X* as long as the other Pi terms are same.

As mentioned earlier, only the propulsive force is considered as head is fixed. In the absence of external forces, propulsive force is being generated by drag on the body and is function of the geometry length of flagella (L), cross section diameter (D), fluid density (ρ), fluid viscosity (μ) and linear velocity (ϑ) as shown in equation (3.4)

$$F_R = f_1(L, D, \rho, \mu, \vartheta), \tag{3.4}$$

Applying the Buckingham Pi theorem, with L, ρ, ϑ as repeating variables instigates as:

$$\pi_1 = \phi(\pi_2, \pi_3) \rightarrow \frac{F_R}{\rho \vartheta^2 L^2} = \phi\left(\frac{\mu}{\rho L \vartheta}, \frac{L}{D}\right) \tag{3.5}$$

This gives the similarity constraints for scaling the suggested system as:

$$\frac{\mu_X}{\rho_X L_X \vartheta_X} = \frac{\mu_Y}{\rho_Y L_Y \vartheta_Y}, \tag{3.6}$$

$$\frac{L_x}{D_x} = \frac{L_y}{D_y} \tag{3.7}$$

$$\frac{F_{RX}}{\rho_X \vartheta_X^2 L_X^2} = \frac{F_{RY}}{\rho_Y \vartheta_Y^2 L_Y^2} \tag{3.8}$$

A test bench of the prototype at any scale can be proposed using the above scaling technique. Then, by amending the other variables of the system and doing scaling accordingly, the test bench system can be utilized to represent a smaller scale system present naturally.

The subsequent section delineates the design of test rig to congregate results on a significant scale prototype of the flexible flagellated nanoswimmer. In the present chapter, the sections are divided to embrace the determination of scaling parameters, the fabrication of flagellated macroswimmer, and the design of test rig to enable propulsive force measurement.

3.2.2 Scaling up of parameters

The first step in designing the test rig is to govern its scale. So as to develop the test bench using conventional manufacturing technique, the geometric parameters of the scaled up flagellated swimmer should be chosen as three thousand times larger than the

natural existing bacteria. Three thousand times scaling factor corresponds to the resulting relationship for the length variable (L):

$$L_Y = 3000 L_X \tag{3.9}$$

The diameter is also scaled up by 3000 times mimicking the natural eukaryotic bacteria and the corresponding relationship for diameter variable (D):

$$D_Y - 3000 D_X \tag{3.10}$$

The Pi terms now can be assessed with the help of available geometric scaling factor to decide the values of system variables. The medium of the system is considered as water in most of the experimental analysis and values of proposed system are:

$$\rho_X = 1000[Kg/m^3],$$
$$\mu_X = 0.001[Pa/s],$$

where, ρ is the fluid density and μ is the fluid medium viscosity. DC motor is connected to elastic tail via scotch yoke mechanism. The speed range and fluid medium is chosen for test rig in such a way to make sure the similarity requirement is endured. To do so, presume that rotational velocity ω and fluid density is similar for both systems. The choice of rotational velocity range is quite controllable which makes the first assumption applicable. The second presumption is also compelling as the density of many fluids varies slightly from that of water. Then equation (3.9) is substituted in equation in (3.6) and the result is reorganized to solve for the test rig fluid viscosity (μ_Y):

$$\mu_Y = \left(\frac{\rho_Y}{\rho_X}\right)\left(\frac{\vartheta_Y}{\vartheta_X}\right)\left(\frac{3000 L_X}{L_X}\right)\mu_X \tag{3.11}$$

As fluid density and speed is equivalent for system X and Y, so it may get cancelled with each other. Hence, viscosity of test rig becomes 3000 times of that of water approximately 3000 cSt. Though, it is also preferred that the fluid be easily available. Therefore, silicon oil having viscosity 350 cSt, 10000 cSt, 15000 cSt and 20000 cSt have been chosen as all are available at the research facility and maintaining low Reynolds regime as mentioned in Table 3.1.

$$\rho_Y = 971[Kg/m^3],$$
$$\mu_Y = 0.3395[Pa.s], 9.71[Pas], 14.57[Pas] and 19.42[Pas]$$

As the silicon oil velocity is not exactly 3000 times that of μ_X, and the two fluid densities are not equivalent, Equation (3.6) must be rearranged to solve for the only unknown left, ϑ_Y.

$$\vartheta_y = \left(\frac{\rho_X}{\rho_Y}\right)\left(\frac{\mu_Y}{\mu_X}\right)\left(\frac{L_X}{3000L_Y}\right)\vartheta_X \tag{3.12}$$

$$\vartheta_Y = 3.333\vartheta_X \tag{3.13}$$

In brief, to indorse the similarity between natural system and test bench, the test bench scale should be 3000 times, is to be run in silicon oil at 333.33% speed. The propulsive force can be evaluated with the help of above defined variables. Equation (3.7) is rearranged to govern the scaling factor for propulsive force:

$$F_{RY} = \left(\frac{971}{1000}\right)\left(\frac{3.33\vartheta_X}{\vartheta_X}\right)^2\left(\frac{3000L_X}{L_X}\right)^2 F_{RX} \tag{3.14}$$

It shows that propulsive forces measured on the test bench are 96905897 times larger than propulsive force generated by natural system. It signifies that the values produced are in the range that is easy to measure.

3.2.3 Importance of Reynolds number

In nature eukaryotic and prokaryotic bacteria utilize rotating helical flagella and beating cilia for their propulsion at micro-scale using molecular motors [7]. At micro/nanoscale robot experiences viscous forces and inertial forces become insignificant. Different propulsion methods for designing micro/ nanoscale robot have been used in liquid [8]. For micro/nanoswimmer and macroswimmer the basic physics such as Reynolds number and Navier stokes equation remains similar. Reynolds number is a dimensionless quantity. It is a defined as the ratio of inertial forces to viscous forces and can be expressed as presented below in equation (3.15)

$$\text{Re} - \frac{\text{Inertial Forces}}{\text{Viscous Forces}} - \frac{\rho v \ell}{\mu} \tag{3.15}$$

where, ρ is the fluid density, v is the fluid velocity, ℓ is dimensional length of the object and μ is dynamic viscosity of fluid. Mostly, micro-organism moves at low Reynolds number regime (less than 10^{-4}) because viscous forces dominate over inertial forces. In 1977, Purcell in his seminal talk "Life at low Reynolds number" stated that at low

Reynolds number environment non-reciprocal motion is required for net displacement [9]. Biological bacteria such as eukaryotic and prokaryotic bacteria swim at Reynolds number less than 1 (Re<<1). Eukaryotic micro-organism such as *spermatozoa* exhibit planar propulsion beat at frequency range 25 Hz to 45 Hz. In the designed test bench, Reynolds number less than 1 is maintained by taking various viscosity of fluid medium and also by controlling the speed of motor. For motor speed 100 RPM, 200 RPM, 300 RPM and 500 RPM and viscosity of fluid is kept in the range of 10000 cSt, 15000 cSt and 20000 cSt as mentioned in Appendix I. The Reynolds number is maintained in the range of 0.0524- 0.5233, which replicate the fluid environment around micro-organisms at scaled up level.

Table 3.1: Value of Reynolds number at different speed in various viscosity of silicon oil

S. No.	SPEED (RPM)	VISCOSITY (cSt)	REYNOLDS NUMBER
1.	100	10000	0.1047
2.	100	15000	0.0698
3.	100	20000	0.05235
4.	200	10000	0.2093
5.	200	15000	0.1395
6.	200	20000	0.1047
7.	300	10000	0.3140
8.	300	15000	0.2093
9.	300	20000	0.1570
10.	500	10000	0.5233
11.	500	15000	0.3489
12.	500	20000	0.2617

3.2.4 DC motor and DC power supply

With the help of the scaling factor, the second part which is to be considered is the motor and the scotch yoke mechanism in the designing of test rig. The test rig uses a geared DC motor (model number: KG152). The motor has maximum torque rating 90

N.cm. Weight of DC motor use in designing of test rig is 85 grams which will be resting on an aluminium cantilever beam. The maximum operating speed is chosen as 100 RPM, 200 RPM, 300 RPM and 500 RPM to fulfill low Reynolds number condition by mimicking micro-organisms. The DC power supply from the laboratory is supplying the 12 V to geared DC motor as shown below in Figure 3.3.

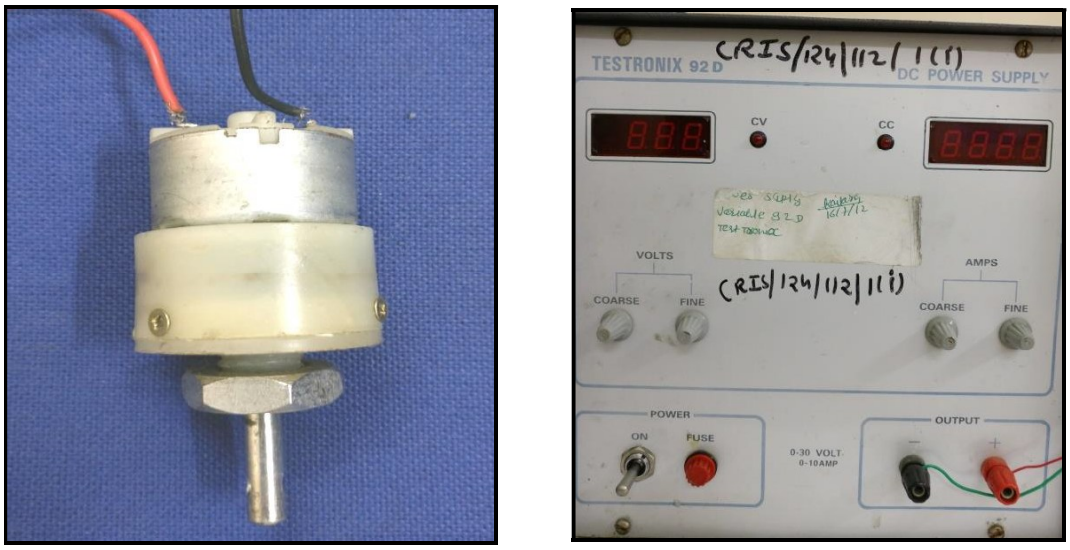

(a) (b)

Figure 3.3: (a) DC motor and (b) DC power supply

3.2.5 Planar propulsion: Scotch Yoke mechanism

In literature, experiments have been performed to oscillate the passive filament via optical tweezer but did not determine the thrust force [10]. Tony et al. have study the shape of tail and measured the thrust force of oscillating filament made up of flexible steel wire [3]. In the present study we also want to oscillate the fabricated branched flagellated artificial swimmer through planar mode of propulsion using scotch yoke mechanism. Scotch yoke mechanism mainly consists of two parts, rolling scotch and sliding yoke (follower). Yoke is compelled by rotor pin placed on the scotch. Forward and backward motion of scotch yoke is synchronously equal [11]. Due to sliding motion of yoke, rotor pin placed eccentrically may wear out early and because of that, pin is fabricated from mild steel which is harder in nature. The scotch yoke and lever mechanism converted the motor's rotation into planar motion of elastic tail.

The scotch yoke consists of rotor pin and follower is shown in Figure 3.4. As motor rotates, the rotor pin follows the circular path. The follower has a slot; whose width matches the diameter of the rotor pin and because of that, the follower obtains the planar motion. The position of follower is altered sinusoidal. The rotor pin is 1 cm away from the center of motor and traces a path through follower with angular velocity 10.47 rad/s, 20.94 rad/s, 31.42 rad/sand 52.33 rad/s for 100 RPM, 200 RPM, 300 RPM and 500 RPM rotating DC motor. Diameter of rotor pin is 5 mm and connected to motor shaft with screw. The follower has same width as rotor pin. Coupler is used to couple flagella with screw to avoid falling of flagella in fluidic chamber as shown in Figure 3.5. Holding screw provide the proper grip to the flagella as shown in Figure 3.5.

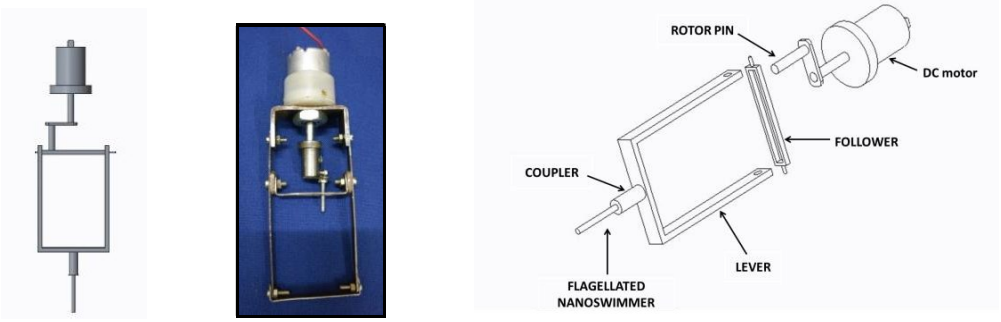

(a) (b) (c)

Figure 3.4: (a) and (b) schematic diagram and designed view of scotch yoke lever mechanism; (c) mentioned each parts of scotch yoke mechanism

In order to investigate the planar wave motion of natural bacteria, we fabricated a scaled up flagellated swimmer which is attached to the scotch yoke mechanism as shown in Figure 3.8(b). The scotch yoke mechanism is connected to DC motor. The motor rotation is converted into planar motion and flagellated swimmer is actuated while base of the flagella is fixed at the origin. The voltage across the DC motor is delivered by the laboratory DC power supply which determines the oscillation frequency. The length of the lever governs the amplitude of oscillation, and at the end of the lever, flagellated swimmer of various design is attached.

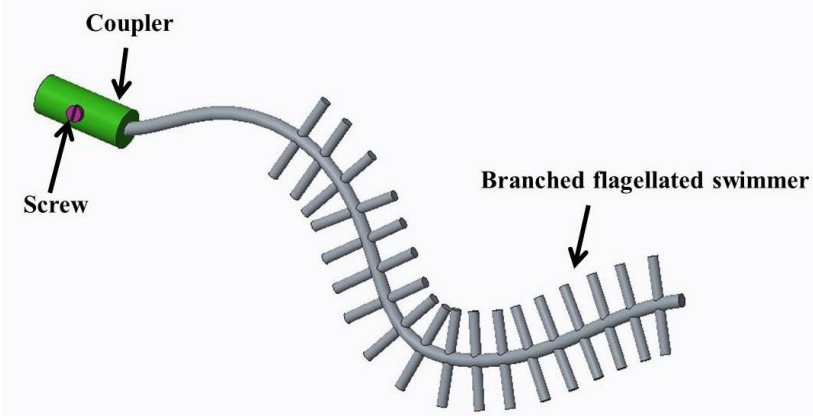

Figure 3.5: Branched flagellated swimmer attached to the coupler through screw

3.3 Mould and Biomimetic Flagellated Macro-swimmer Fabrication Process

The prime aim of the present research work is to fabricate the branched flagellated swimmer by mimicking *Ochromonas malhamensis* as shown in Figure 3.6. In nature *Ochromonas malhamensis* bears vertical appendages (mastigonemes) on flagella that locomote along with flagella in same direction and thrust force is mostly dominated by mastigonemes [12]. It has been observed that due to presence of mastigonemes effective surface area increases leads to increase in the thrust force generated by main flagella [13]. In Figure 3.6(b), illustration of *ochromonas* bearing mastigonemes have been presented. L and D are the length and diameter of flagella, whereas l and d are length and diameter of branches on flagella surface and S is the spacing between two consecutive branches on flagella. Length of branches is kept same through the length of flagella. Cilia of various length, width and spacing of various shapes such as T-shaped, L-shaped, triangular shaped, rectangular shaped and structure containing holes have been fabricated till date to study the effect of parameters of artificial cilia under applied magnetic-field [14]. Researchers are now designing artificial biological swimmer that can mimic flagella/cilia-powered swimming in 2D through computational simulation work [15], [16]. Till now working principle of flagella and cilia is utilized to design artificial microswimmer [17]-[19] for fluid flow and mixing of fluid at micron level [20]-[22] while flagella bearing hair like structures known as mastigonemes (Figure 3.6(a)) is not studied much. We have bio-mimicked the structure of genus algae *Ochromonas*. In literature, cilia are actuated by external field such as piezo actuation, light, magnetic [23], [24] and electrostatic while investigation of the enhancement in propulsive force of

planar mode propulsion of branched flagellated swimmer at scaled up level is carried out in present thesis.

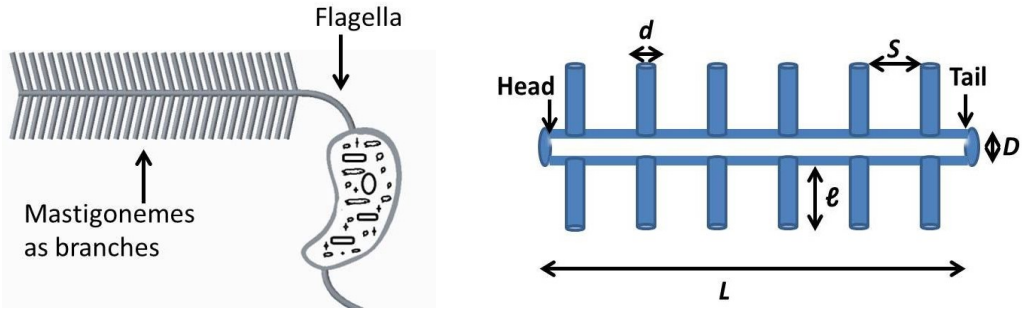

(a) (b)

Figure 3.6: (a) Image of genus algae *Ochrophyte* [25] and (b) illustration of flagella having mastigonemes. L and D are the length and diameter of flagellum, whereas ℓ, d and S are height, diameter of mastigonemes known as branches in our work and S is the spacing between branches (mastigonemes)

3.3.1 Moulds of branched flagella

Various moulds have been designed and machined in workshop. Mould material is chosen as aluminum because machining can be done easily on it with the help of lathe machine. It offers many advantages such as low cost, versatile, adaptability and light in weight and nontoxic so can be used safely in fabrication of biological swimmer. Mould is shown in Figure 3.7 for flagellated swimmer. The dimensions of mould are chosen as per the design of flagellated swimmer [26]. Because of its softness, it can be easily machined eight times faster than steel [27]. Aluminum mould has certain disadvantages also it can be dented easily on excessive pressure or by detaching part through sharp object [28]. By proper handling and caring of steel moulds it can last longer even aluminum mould can be seen as more artistic and creative than standard steel [26]. It is decided to investigate three designs of scaled up flagellated swimmer. First; branches on flagellated swimmer is kept at 90° (straight branches) as mastigonemes on flagella in *Ochromonas* and secondly branches are kept at 60° and in third case 120° orientation of branches are done on flagella surface. Details of these designs of branched flagellated swimmer by varying parameters are discussed in Chapter 4. A mould of branches at 90° on flagella design is fabricated first to make sure the shape of design is precise as shown below in Figure 3.7.

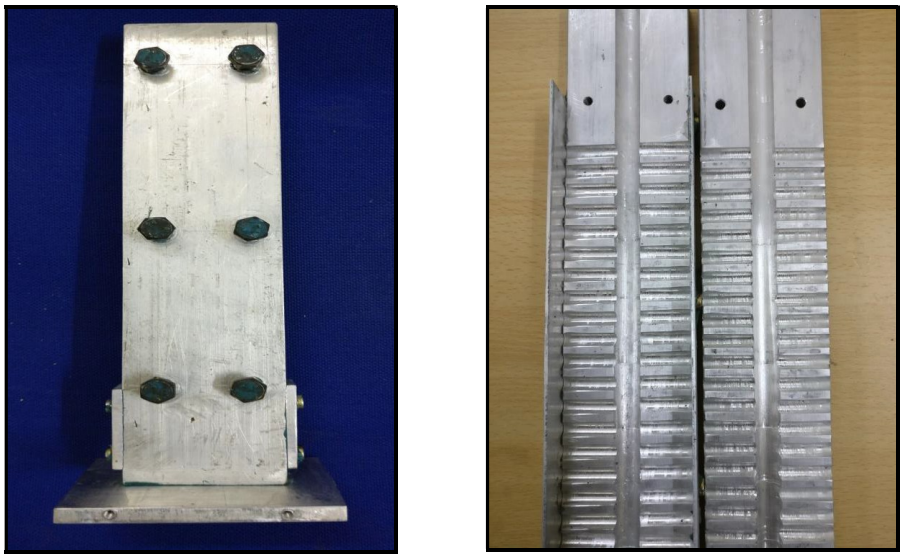

(a) (b)

Figure 3.7: Aluminium mould in (a) closed position and (b) open positions with branches at 90° on flagella

3.3.2 Prerequisite of nanoswimmer: Biocompatible material of fabricated flagella

Due to recent advancement in the field of nanotechnology, there is a growing literature available on nanorobot. Accordingly, the possibility of inspecting human body using nanorobots is inexorability. Various parts of human body filled with fluid need to explore such as renal system, eyeball and circulatory system. Therefore, there prevails a need to exploit an innocuous, efficient locomotion system for swimming *in-vivo*. Locomotion of nanorobot for *in-vivo* applications possess some limitations which is described in the given section. They are enumerated in qualitative terms to keep in mind the design concept.

Biocompatibility can be described as the potential of material or system not to produce harmful effect in the human environment it is working on. The introduction of any foreign body such as nanorobots can be really challenging because it needs to work without any chemical reaction and immune system response inside the human body environment. More imperative solution is to employ biomaterials, it allows material scientist to synthesize biocompatible polymer to utilize them in numerous scientific area such as drug delivery, tissue engineering and wound dressing etc. Biomaterials should not adhere to the cell unless it is intended to do so. It should not produce biological effect such as toxicity, infection. Physical and mechanical effects of body should not get

disturb due to implant. Nano-device should able to work in different acidic and viscosity environment. In literature few materials have been noted down as biocompatible material such as polydimethylsiloxane (PDMS) [29], polyvinylidenefluoride (PVDF), polyethylene (PE) and cellulose acetate (CA) [30] suitable for biomedical applications. PDMS is in use long back for microfluidic applications as well as in BIOMEMS [31]. We can also utilize its flexible nature for designing flagellated nanoswimmer of various shapes. Till now researchers have attempted experiments by designing swimmers of rigid materials mostly copper wire [32],[33], steel wire [34],[35], steel spring [6], NdFeB/Tungsten wire [2], NdFeB/Polyurethane/PDMS [36]. Design of macro-swimmer made up of flexible PDMS polymer is not attempted yet. So, the flagellated swimmer is fabricated from flexible PDMS biocompatible material. The biomimetic branched flagellated swimmer with branches oriented at 90° fabricated from PDMS is shown in Figure 3.8(b). The dimensions of the fabricated branched flagella are scaled up with approximately 3000 times of the paramecium to make easier the fabrication procedure and to maintain low Reynolds number regime. The geometric parameters chosen for fabrication of branched flagella; the dimensions of branches are length-20 mm and diameter- 5 mm whereas the dimensions of flagella are length- 150 mm and diameter-10mm at scaled up level. The branches have been taken symmetrical on both sides of cylindrical flagella as shown in Figure 3.8.

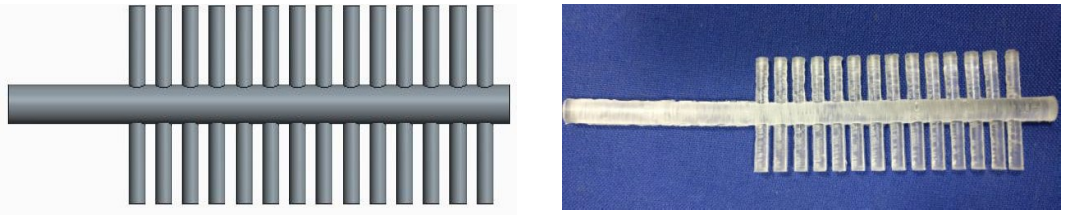

(a) (b)

Figure 3.8: Fabricated branches (a) schematic diagram and (b) branches at 90° on flagella using PDMS material by mimicking *Ochromonas* algae genus

The material used for fabricating flexible scaled up flagellated swimmer is purchased from Dow corning silicone elastomer (sylgard 184). The fabricated branched flagellated swimmer is combination of two liquids; one is pre polymer base (elastomer) and second is cross linking curing agent (shown in Appendix I), when combined get solidify. It can be cured at room temperature as well as temperature shall be increased up to 200° C to cure for particular time interval. The sample is mixed properly for some time. The

PDMS mixture was then poured into aluminium mould. The mould filled with PDMS is then kept inside the oven at 125° C temperature for 20 minutes as reported in the literature [37]. The curing time and temperature is taken as per recommended by Dow corning. The oven is preheated to 125° C before putting sample inside it. The elastomer and curing agent mix well in 10:1 ratio. PDMS is most commonly biocompatible material used for microfluidic applications. It displays various advantages such as easy to fabricate, transparent, low cost and less shrinkage over the time [37].

3.4 Experimental set-up for Planar Propulsion of Branched PDMS Flagella

A fabricated PDMS flagellated macroswimmer is immersed in high viscosity silicon oil to mimic low Reynolds number environment experienced by microorganism. The branches and flagella both are fabricated in cylindrical shape using PDMS (Young's modulus-2.46MPa) biocompatible material purchased from Dow corning. The cantilever beam hold the motor connected to branched flagella with scotch yoke lever mechanism. The cantilever beam is made of aluminium shown in Appendix I. Flagellum is fastened with scotch yoke mechanism to experience planar motion. In comparison to Tony et al. [3] design set up for planar propulsion, we submerged flagella vertically with respect to bottom because it is flexible in nature and flagella will deflect easily. Propulsive force generated by flagellar planar propulsion is calculated by measuring deflection of cantilever beam through laser micrometer. The schematic of experimental set up is shown in Figure 3.9(a). Test rig of flexible flagellated swimmer designed at scaled up level is shown in Figure 3.9(b). The base of the flagella is connected to the mild steel lever coupler as shown in Figure 3.5. A set of screw embraces the flagella to the motor with the help of scotch yoke lever. The experiments have been conducted in silicon oil medium having viscosity 350 cSt, 10000 cSt, 15000 cSt and 20000 cSt and motor speed is kept 100 RPM, 200 RPM, 300 RPM and 500 RPM to maintain low Reynolds number (Re≈1) flow condition. Data of deflection of cantilever beam is recorded for 512 sec through Keyence laser micrometer. The time varying deflection is experienced by cantilever beam due to planar motion of branched flagella. The scotch yoke mechanism translates rotational motion into linear motion to engender planar wave movement of attached flagella. The cantilever beam is deflected due to propulsive force generated by planar propulsion of branched flagella in viscous medium which is measured by Keyence LS-7601 laser micrometer.

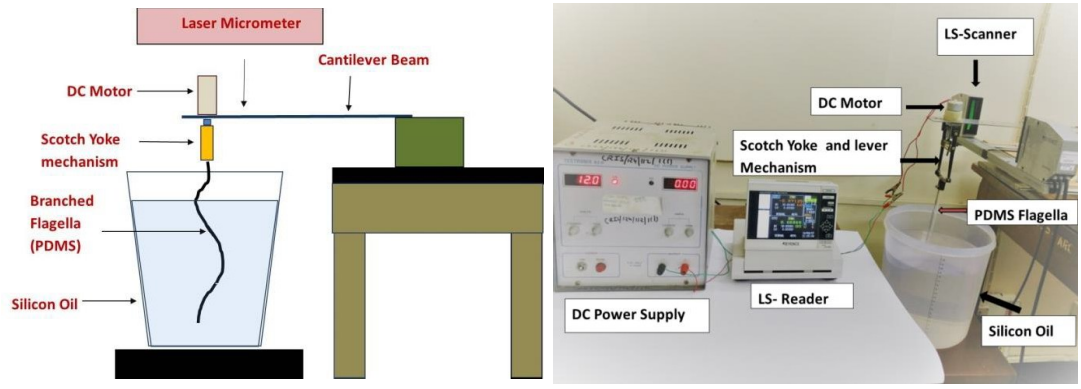

(a) (b)

Figure 3.9: (a) Showing schematic diagram and (b) test rig designed at scaled up level for flagellated nanoswimmer

3.4.1 Deflection measurement of cantilever beam act as transducer

Lase Micrometer is used to scan the point of deflection at bottom and top surface of cantilever beam by intersecting the laser light passed through it. The measured values on controlled panel can be directly observed and recorded in real time on computer. The values on OUT 1 display and OUT 2 display are showing the deflection value on upper and lower surface of cantilever beam. Before taking readings or start measurements the values on display can be reset to zero using zero button and measurement get started after pressing run button. The measured value taken from the controller is directly transferred to an excel sheet. The recorded data is then further processed for analysis. The measurement is recorded in millimetres. The control panel is shown below in Figure 3.10.

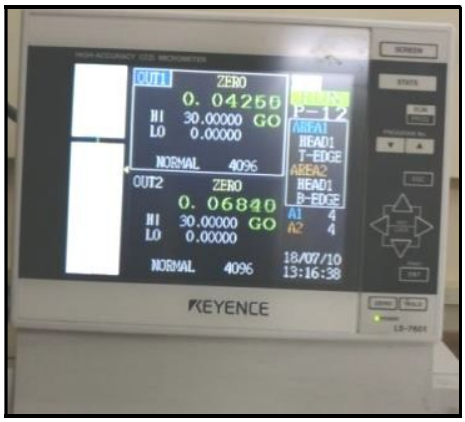

Figure 3.10: Displaying output of deflection of cantilever beam due to thrust force generated by planar motion of flagellated swimmer

Whenever experimentation instigated each time, laser micrometre is ON and then zeroed. The flagellum is run at given RPM for several minutes to attain steady state after that data acquisition initiate. After each run the laser micrometer is reset and test begin again. The result is a response of deflection time history towards free end of cantilever beam on which motor is connected and whose rotational motion is converted into planar propulsion via scotch yoke lever mechanism. The effect of branches in terms of deflection of cantilever beam is recorded. Each branched flagella has uniform diameter throughout the length and is made up of linearly elastic, biocompatible PDMS material.

3.4.2 Propulsive force measurement procedure

To measure propulsive force of flagellated swimmer, a cantilever beam along with laser micrometer is used. Flagellated swimmer along with scotch yoke mechanism, fixed at free end of the cantilever beam having thickness 1.86 mm. The motor rotation is converted into linear motion by scotch yoke mechanism. The planar motion of swimmer will lead to thrust force generation which is exerted on the tip of the beam and deflects the beam. Laser micrometer set near the cantilever beam fixed end at a distance 129 mm from free end and will measure and record the deflection value. The resulting deflection value is then converted into force value by applying beam theory.

If a propulsive force is applied at the tip of a cantilever beam of length *L*, thickness *t* and width *w*, then deflection x at position '*a*' is shown in Figure 3.11. Propulsive force is calculated by equation (3.16) through measuring deflection at point '*a*' through laser micrometer.

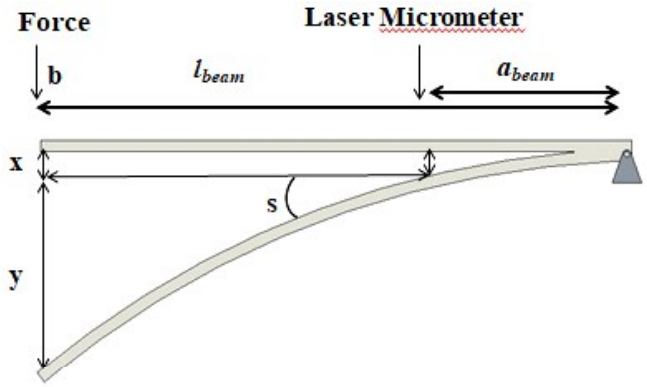

Figure 3.11: Showing beam diagram to calculate thrust force generated at tip of cantilever beam

Propulsive Force:
$$F_{LS} = \frac{\delta_{beam} \times E_{beam} \times I_{beam}}{\left[\frac{(l_{beam} - a_{beam})^3}{6} + \frac{l_{beam}^2 \times a_{beam}}{2} - \frac{l_{beam}^3}{6}\right]} \quad (3.16)$$

where E (69 GPa) is the Young's modulus of aluminium cantilever beam and I is moment of inertia of rectangular cross section beam. 'a_{beam}' is the distance where Laser micrometer is installed and deflection δ_{beam} (in millimetre) of cantilever beam is measured and respectively propulsive force 'F_{LS}' is calculated. Due to planar motion of flagella cantilever beam is deflected at point *'b'*. By this, propulsive force generated due to planar motion of flagellated swimmer inside the silicon oil of different viscosity is calculated. At initial, the test rig should be at resting position. The cantilever beam is rigid enough so that beam will not lift and bend from its static position. Two points are considered while taking propulsive force measurement; first, at rest propulsive force is equal to zero. Second, when motor is on the flagellated swimmer generates a propulsive force. The weights of all the parts of test rig remain same at both point of interest. Propulsive force for different designs of branched flagellated swimmer is calculated by laser-micrometer deflection value in different environmental condition.

3.5 Summary

This chapter demarcate the design procedure to develop the propulsion system of branched flagellated swimmer at scaled up level suitable for human body environment. This incorporates describing the need, detailing the design concept, design constriction (biocompatibility, Reynolds number) and feasible solution to the problem. In the next chapter design of experiment (DOE) approach is utilized to study the effect of number of branches and orientation of branches along with spacing between two consecutive branches. The effects of above mentioned parameters of branched flagella in terms of propulsive force will be examined through statistical methodology.

References:

[1] J. S. Rathore and N. N. Sharma, *Engineering Nanorobots : Past , present and future perspectives*. CRC Concise Encyclopedia of Nanotechnology, Taylor and Francis, pp. 1-54, 2015.

[2] L. Wang, H. Xu, W. Zhai, B. Huang, and W. Rong, "Design and Characterization of Magnetically Actuated Helical Swimmers at Submillimeter-scale," *Journal of Bionic Engineering*, vol. 14, no. 1, pp. 26–33, 2017.

[3] S. Y. Tony, E. Lauga, and A. E. Hosoi, "Experimental investigations of elastic tail propulsion at low Reynolds number," *Physics of Fluids (1994-present)*, vol. 18, no. 9, pp. 91701-91705, 2006.

[4] B. Behkam and M. Sitti, "Design methodology for biomimetic propulsion of miniature swimming robots," *Journal of Dynamic Systems, Measurement, and Control*, vol. 128, no. 1, pp. 36–43, 2006.

[5] U. Danis, R. Rasooli, C.-Y. Chen, O. Dur, M. Sitti, and K. Pekkan, "Thrust and Hydrodynamic Efficiency of the Bundled Flagella," *Micromachines*, vol. 10, no. 7, pp. 449–470, 2019.

[6] J. Singleton, E. Diller, T. Andersen, S. Regnier, and M. Sitti, "Micro-scale propulsion using multiple flexible artificial flagella," in *Intelligent Robots and Systems (IROS), 2011 IEEE/RSJ International Conference on*, pp. 1687–1692, 2011.

[7] H. C. Berg and R. A. Anderson, "Bacteria swim by rotating their flagellar filaments," *Nature*, vol. 245, no. 5425, pp. 380–382, 1973.

[8] F. Qiu and B. J. Nelson, "Magnetic helical micro-and nanorobots: Toward their biomedical applications," *Engineering*, vol. 1, no. 1, pp. 21–26, 2015.

[9] E. M. Purcell, "Life at low Reynolds number," *American journal of physics*, vol. 45, no. 1, pp. 3–11, 1977.

[10] C. H. Wiggins, D. Riveline, A. Ott, and R. E. Goldstein, "Trapping and wiggling: elastohydrodynamics of driven microfilaments," *Biophysical Journal*, vol. 74, no. 2, pp. 1043–1060, 1998.

[11] E.-C. Lovasz *et al.*, "Novel design solutions for fishing reel mechanisms," *Chinese Journal of Mechanical Engineering*, vol. 28, no. 4, pp. 726–736, 2015.

[12] H. Guo, J. Nawroth, Y. Ding, and E. Kanso, "Cilia beating patterns are not hydrodynamically optimal," *Physics of Fluids*, vol. 26, no. 9, pp. 91901-91913, 2014.

[13] S. Tottori and B. J. Nelson, "Artificial helical microswimmers with mastigoneme-inspired appendages," *Biomicrofluidics*, vol. 7, no. 6, pp. 61101-61106, 2013.

[14] J. Belardi, N. Schorr, O. Prucker, and J. Rühe, "Artificial cilia: generation of magnetic actuators in microfluidic systems," *Advanced Functional Materials*, vol. 21, no. 17, pp. 3314–3320, 2011.

[15] S. N. Khaderi and P. R. Onck, "Fluid–structure interaction of three-dimensional magnetic artificial cilia," *Journal of Fluid Mechanics*, vol. 708, pp. 303–328, 2012.

[16] A. Babataheri, M. Roper, M. Fermigier, and O. Du Roure, "Tethered fleximags as artificial cilia," *Journal of Fluid Mechanics*, vol. 678, pp. 5–13, 2011.

[17] P. Tierno, R. Golestanian, I. Pagonabarraga, and F. Sagués, "Magnetically actuated colloidal microswimmers," *The Journal of Physical Chemistry B*, vol. 112, no. 51, pp. 16525–16528, 2008.

[18] A. Ghosh and P. Fischer, "Controlled propulsion of artificial magnetic nanostructured propellers," *Nano letters*, vol. 9, no. 6, pp. 2243–2245, 2009.

[19] J. J. Abbott *et al.*, "How should microrobots swim?," *The international journal of Robotics Research*, vol. 28, no. 11–12, pp. 1434–1447, 2009.

[20] S. N. Khaderi, M. Baltussen, P. D. Anderson, D. Ioan, J. M. J. Den Toonder, and P. R. Onck, "Nature-inspired microfluidic propulsion using magnetic actuation," *Physical Review E*, vol. 79, no. 4, pp. 46301-46304, 2009.

[21] S. N. Khaderi *et al.*, "Magnetically-actuated artificial cilia for microfluidic propulsion," *Lab on a Chip*, vol. 11, no. 12, pp. 2002–2010, 2011.

[22] J. den Toonder *et al.*, "Artificial cilia for active micro-fluidic mixing," *Lab on a Chip*, vol. 8, no. 4, pp. 533–541, 2008.

[23] D. Isvoranu, D. Ioan, and P. Parvu, "Kinematics and flow characteristics of a magnetic actuated multi-cilia configuration," *Medical engineering & physics*, vol. 33, no. 7, pp. 868–873, 2011.

[24] S. N. Khaderi, J. M. J. Den Toonder, and P. R. Onck, "Magnetically actuated artificial cilia: The effect of fluid inertia," *Langmuir*, vol. 28, no. 20, pp. 7921–7937, 2012.

[25] S. Namdeo, S. N. Khaderi, J. M. J. den Toonder, and P. R. Onck, "Swimming direction reversal of flagella through ciliary motion of mastigonemes," *Biomicrofluidics*, vol. 5, no. 3, pp. 34108-34124, 2011.

[26] "Why Offer Aluminum Molds for Production MoldMaking Technology." [Online]. Available: https://www.moldmakingtechnology.com/articles/why-offer-aluminum-molds-for-production.

[27] "The Best Aluminum Alloys For Molds Clinton Aluminum." [Online]. Available: https://www.clintonaluminum.com/the-best-aluminum-alloys-for-molds/.

[28] "Advantages of Aluminum Production Molds _ Midwest Mold." [Online]. Available: http://midwestmold.com/advantages-of-aluminum-production-molds/.

[29] B. A. Evans, A. R. Shields, R. L. Carroll, S. Washburn, M. R. Falvo, and R. Superfine, "Magnetically actuated nanorod arrays as biomimetic cilia," *Nano letters*, vol. 7, no. 5, pp. 1428–1434, 2007.

[30] R. Majumdar, N. Singh, J. S. Rathore, and N. N. Sharma, "In search of materials for artificial flagella of nanoswimmers," *Journal of Materials Science*, vol. 48, no. 1, pp. 240–250, 2013.

[31] E. Sollier, C. Murray, P. Maoddi, and D. Di Carlo, "Rapid prototyping polymers for microfluidic devices and high pressure injections," *Lab on a Chip*, vol. 11, no. 22, pp. 3752–3765, 2011.

[32] T. Honda, K. I. Arai, and K. Ishiyama, "Micro swimming mechanisms propelled

by external magnetic fields," *Magnetics, IEEE Transactions on*, vol. 32, no. 5, pp. 5085–5087, 1996.

[33] F. Z. Temel, A. E. Bezer, and S. Yesilyurt, "Navigation of mini swimmers in channel networks with magnetic fields," in *Robotics and Automation (ICRA), 2013 IEEE International Conference on*, pp. 5335–5340, 2013.

[34] B. Behkam and M. Sitti, "Modeling and testing of a biomimetic flagellar propulsion method for microscale biomedical swimming robots," in *IEEE Advanced Intelligent Mechanotronics Conference, Monterey, CA*, pp. 24–28, 2005.

[35] A. G. Erman and S. Yesilyurt, "Swimming of onboard-powered autonomous robots in viscous fluid filled channels," in *Mechatronics (ICM), 2011 IEEE International Conference on*, pp. 348–353, 2011.

[36] Z. Ye, S. Régnier, and M. Sitti, "Rotating Magnetic Miniature Swimming Robots With Multiple Flexible Flagella," *IEEE Transactions on Robotics*, vol. 30, no. 1, pp. 3–13, 2014.

[37] I. D. Johnston, D. K. McCluskey, C. K. L. Tan, and M. C. Tracey, "Mechanical characterization of bulk Sylgard 184 for microfluidics and microengineering," *Journal of Micromechanics and Microengineering*, vol. 24, no. 3, pp. 35017-35024, 2014.